

# Fluctuation-Induced Heat Release from Temperature-Quenched Nuclear Spins near a Quantum Critical Point

Y. H. Kim,<sup>1</sup> N. Kaur,<sup>2</sup> B. M. Atkins,<sup>3</sup> N. S. Dalal,<sup>2</sup> and Y. Takano<sup>1</sup>

<sup>1</sup>*Department of Physics, University of Florida, P.O. Box 118440, Gainesville, Florida 32611-8440, USA*

<sup>2</sup>*Department of Chemistry and Biochemistry, Florida State University, Tallahassee, FL 32306, USA*

<sup>3</sup>*Department of Physics, Rhodes College, Memphis, TN 38112, USA*

(Dated: November 8, 2018)

At a quantum critical point (QCP) — a zero-temperature singularity in which a line of continuous phase transition terminates — quantum fluctuations diverge in space and time, leading to exotic phenomena that can be observed at non-zero temperatures. Using a quantum antiferromagnet, we present calorimetric evidence that nuclear spins frozen in a high-temperature nonequilibrium state by temperature quenching are annealed by quantum fluctuations near the QCP. This phenomenon, with readily detectable heat release from the nuclear spins as they are annealed, serves as an excellent marker of a quantum critical region around the QCP and provides a probe of the dynamics of the divergent quantum fluctuations.

PACS numbers: 75.30.Kz, 75.40.-s, 75.50.Ee, 76.60.Es

Quantum criticality, the divergence of spatial and temporal extents of quantum fluctuations at a continuous phase transition at zero temperature, is the driving mechanism behind a variety of novel phenomena that challenge conventional theoretical approaches to collective behavior of many-body systems and may also lead to technological applications [1, 2]. This criticality is responsible for the breakdown of Fermi-liquid behavior in heavy-fermion metals [3, 4] and for the emergence of exotic states of matter such as unconventional superconductors [5, 6], nematic electron fluids [7] in GaAs/AlGaAs heterojunctions [8] and Sr<sub>3</sub>Ru<sub>2</sub>O<sub>7</sub> [9], and yet-to-be-identified ‘reentrant hidden-order’ states in URu<sub>2</sub>Si<sub>2</sub> [10].

Unlike in classical criticality, which is the divergence of order-parameter fluctuations in space at a continuous phase transition occurring at a non-zero temperature [11], dynamic and static properties are inextricably linked in quantum criticality [12, 13]. A spectacular demonstration of this linkage is the quantum annealing — the quantum-fluctuation-driven relaxation of quenched disorder — of an Ising spin glass near its quantum critical point (QCP), a phenomenon with broad implications in efficient optimization algorithms [14, 15]. Here we report the finding of another relaxation phenomenon near a QCP: quantum-fluctuation-driven release of heat from nuclear spins. This finding opens up a unique avenue to investigate the dynamics of quantum fluctuations that underlie quantum criticality.

For this study, we have chosen the inorganic coordination compound Cr(diethylenetriamine)(O<sub>2</sub>)<sub>2</sub>·H<sub>2</sub>O, hereafter referred to as Cr(dien), because of its large number of hydrogen nuclear spins [16, 17]. This quasi-two-dimensional quantum magnet has a magnetic-field-tuned QCP at the field  $H_c = 12.3$  T, where a highly polarized antiferromagnetic phase gives way to a field-induced ferromagnetic phase. The Cr(diethylenetriamine)(O<sub>2</sub>)<sub>2</sub> molecule, the key building block of this material, is an

oblate, elongated disk-shaped molecule illustrated in Fig. 1(a). The magnetic ion is Cr(IV), located on the mirror-symmetry plane of the molecule. In the monoclinic crystal structure of Cr(dien), the  $S = 1$  spins of Cr(IV) form a square lattice along the crystallographic  $ac$  plane, with an exchange energy  $J$  of 2.71–2.88 K. The spins order antiferromagnetically at  $T_N = 2.55$  K in zero magnetic field [17]. Application of a high magnetic field depresses the ordering temperature, pushing it to zero at the critical field  $H_c$ . We work near this QCP.

The experiment is done in a relaxation calorimeter [18, 19]. A 1.02 mg single crystal of Cr(dien) is placed on the sample platform, weakly linked to the thermal reservoir through the leads for the thermometer and heater. This geometry allows the sample temperature to be raised with ease and to drop rapidly to the reservoir temperature when the heater is turned off. It also enables the detection of spontaneously released heat in the sample as an observable temperature difference between the sample and the reservoir.

The procedure of the experiment is illustrated in Fig. 1(b). First, the sample is heated from temperature  $T_0$  (point  $P_1$  or  $P'_1$  in the figure) of the thermal reservoir to temperature  $T_q$  (point  $P_2$  or  $P'_2$ ) ranging from 266 mK to 1.52 K, in magnetic field  $H_q$  applied perpendicular to the  $ac$  plane of the crystal. After 1.4 min at  $T_q$ , the sample is rapidly cooled back to  $T_0$  in 1.8 s by turning off the heater. This temperature quenching leaves the hydrogen nuclear spins frozen in a nonequilibrium high-energy state corresponding to  $T_q$ . Subsequently, the magnetic field is swept at 0.2 T/min or 0.1 T/min through the critical field  $H_c$ . The field sweeps are made at four different  $T_0$  ranging from 96 mK to 261 mK.

As the swept field approaches  $H_c$ , heat is released in the sample, manifesting itself as a pronounced peak in the temperature difference  $\Delta T$  between the sample and the thermal reservoir, as shown in Figs. 1(c) and 1(d).

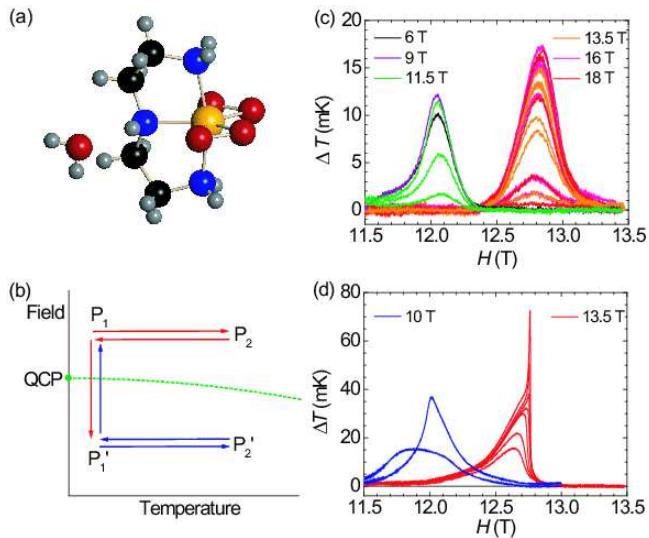


FIG. 1: (color online). (a) Pair of  $\text{H}_2\text{O}$  and  $\text{Cr}(\text{diethylenetriamine})(\text{O}_2)_2$  molecules, the basic unit of the  $\text{Cr}(\text{dien})$  crystal. The  $\text{Cr}(\text{IV})$  ion is the largest sphere to the right, bonded to four oxygen and three nitrogen atoms. (b) Procedure of the experiment (see text). Broken line, terminating in a quantum critical point at  $T = 0$ , is the boundary between the highly polarized paramagnetic phase and antiferromagnetic phase. (c) Temperature difference  $\Delta T$  between the sample and the thermal reservoir as a function of the magnetic field during field sweeps at  $0.2 \text{ T/min}$ . The thermal reservoir is held at  $181 \text{ mK}$ . Temperature  $T_q$  from which the sample has been quenched ranges from  $266 \text{ mK}$  to  $1.52 \text{ K}$ . (d) Evolution of  $\Delta T$  when the thermal reservoir is held at  $96 \text{ mK}$ , as the field is swept at  $0.1 \text{ T/min}$ .  $T_q$  ranges from  $300 \text{ mK}$  to  $797 \text{ mK}$ . In (c) and (d), the peaks to the right are observed during downward field sweeps and those to the left during upward sweeps. The fields indicated in the legends are  $H_q$ .

The heat release occurs only during the first field sweep after the temperature quenching of the sample from  $T_q$ , not during subsequent sweeps [20].

The amount of released heat  $Q$  is obtained from the data via

$$Q = \int \kappa \Delta T dH / \dot{H}, \quad (1)$$

where  $\kappa$  is the thermal conductance of the weak link between the sample and the thermal reservoir, and  $\dot{H}$  the field-sweep rate. As shown in Figs. 2(a) and 2(b),  $Q$  depends on  $T_q$ ,  $H_q$ , and  $T_0$ . These dependences indicate unambiguously that the heat is indeed released from the hydrogen nuclear spins, as the following analysis reveals.

When hydrogen nuclear spins in magnetic field  $H_q$  are initially frozen in a nonequilibrium high-energy state determined by temperature  $T_q$  — while the lattice cools rapidly to temperature  $T_0$  — and subsequently equilibrate with the lattice at another field  $H$ , the amount of

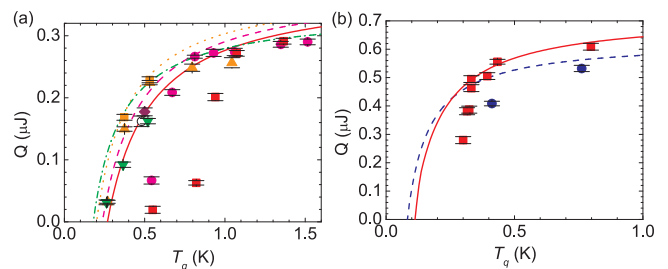


FIG. 2: (color online). Amount of heat released at (a)  $181 \text{ mK}$  and (b)  $96 \text{ mK}$  as a function of  $T_q$ , the temperature from which the sample has been rapidly quenched. In (a), the sample has been quenched at  $H_q = 6 \text{ T}$  ( $\circ$ ),  $9 \text{ T}$  ( $\blacklozenge$ ),  $11.5 \text{ T}$  ( $\blacktriangledown$ ),  $13.5 \text{ T}$  ( $\blacktriangle$ ),  $16 \text{ T}$  ( $\bullet$ ), and  $18 \text{ T}$  ( $\blacksquare$ ). The lines represent Eq. 2 with  $n_H = 10$ : dash-dotted line for  $H_q = 11.5 \text{ T}$ , dotted line  $13.5 \text{ T}$ , broken line  $16 \text{ T}$ , and solid line  $18 \text{ T}$ . In (b), the sample has been quenched at  $10 \text{ T}$  ( $\bullet$ ) and  $13.5 \text{ T}$  ( $\blacksquare$ ). The lines representing Eq. 2 are with  $n_H = 10$  for  $H_q = 10 \text{ T}$  (broken line) and with  $n_H = 15$ , of which five are assumed to freeze only at  $132 \text{ mK}$ , for  $13.5 \text{ T}$  (solid line.)

heat released by them is

$$Q = n_H n R \left( \frac{\hbar \gamma}{k_B} \right)^2 \frac{I(I+1)}{3} \left( \frac{H}{T_0} - \frac{H_q}{T_q} \right) H. \quad (2)$$

Here  $n_H$  is the number of hydrogen nuclear spins (per formula unit) that participate in heat release,  $n$  sample's mole number,  $R$  the gas constant,  $\hbar$  the Planck constant,  $k_B$  the Boltzmann constant, and  $\gamma$  and  $I = 1/2$  the gyromagnetic ratio and spin of the hydrogen nucleus. The equation takes into account that the nuclear-spin temperature just before the heat release is  $HT_q/H_q$  instead of  $T_q$ , as a result of the field sweep from  $H_q$  to  $H$  being adiabatic for the nuclear spins except very near  $H$ .

For  $T_0 = 181 \text{ mK}$ , good agreement between experiment and Eq. 2 is obtained with  $n_H = 10$ , as shown in Fig. 2(a), except for a few points for which  $H_q$  is  $18 \text{ T}$  or  $16 \text{ T}$  [21]. At  $T_0 = 96 \text{ mK}$ , the peak that appears at  $12.76 \text{ T}$  in Fig. 1(d) during downward field sweeps from  $13.5 \text{ T}$  is very sharp while  $\Delta T > 36 \text{ mK}$ , *i.e.*, while the sample temperature  $T_0 + \Delta T$  is higher than  $132 \text{ mK}$ . This indicates that hydrogen nuclear spins whose relaxation times  $\tau$  are very short when  $T_0 > 132 \text{ mK}$  now participate in heat release. When  $T_0 = 181 \text{ mK}$ , they have evidently reached thermal equilibrium with the lattice before each field sweep starts and therefore do not participate in heat release. As shown in Fig. 2(b), good agreement between Eq. 2 and the  $T_0 = 96 \text{ mK}$  data for  $H_q = 13.5 \text{ T}$  is obtained with  $n_H = 15$ , of which five whose  $\tau$  are very short at  $T_0 > 132 \text{ mK}$  are assumed to freeze at a nonequilibrium high-energy state at  $132 \text{ mK}$  instead of  $T_q$ . When quenched at  $H_q = 10 \text{ T}$ , in the antiferromagnetic phase,  $n_H = 10$  gives better agreement with the data, suggesting that those five hydrogen nuclear spins do not participate in heat release even at  $T_0 = 96 \text{ mK}$ .

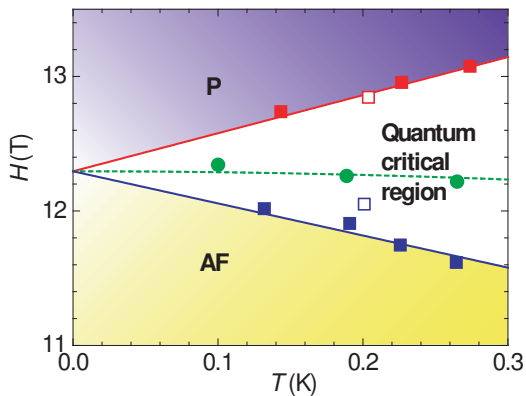


FIG. 3: (color online). Magnetic fields and temperatures of the peaks in the  $\Delta T$  curves (squares), marking a quantum critical region delimited by two straight lines through the data points. Solid squares are for peaks at a sweep rate of 0.1 T/min, open squares at 0.2 T/min. Circles represent the phase boundary — detected by the magnetocaloric effect — between the antiferromagnetic (AF) and highly polarized paramagnetic (P) phases, with the broken line from a power-law fit of data points up to 0.84 K. At zero temperature, the P phase turns into a field-induced ferromagnetic phase.

Cr(dien) contains fifteen hydrogen atoms per formula unit, as shown in Fig. 1(a). Among the thirteen in the Cr(diethylenetriamine)(O<sub>2</sub>)<sub>2</sub> molecule, the five bonded to nitrogens are closer to the Cr(IV) ion than eight that are bonded to carbons [22]. It is very likely that the five hydrogens with short nuclear-spin  $\tau$  are those bonded to the nitrogens and thus experience stronger fluctuating dipolar field and transferred hyperfine field of the Cr(IV) ion, whereas the ten hydrogens with longer  $\tau$  are those bonded to the carbons and the two in the water molecule.

The positions of the heat-release peaks [23] are shown in Fig. 3 along with the phase boundary between the highly polarized antiferromagnetic phase and similarly highly polarized paramagnetic phase, which turns into the field-induced ferromagnetic phase at zero temperature, of Cr(dien) near its QCP at  $H_c$ . This diagram suggests that, in the zero-temperature limit, the loci of the peaks converge on the QCP. These loci delimit the region in which  $\tau$  is shorter than the timescale of the experiment, a quantum critical region.

How does  $\tau$  vary within and near this region? To answer this question, we stop the field sweep at field  $H$  and record the subsequent relaxation of the sample temperature toward  $T_0$  [24]. The measurements are carried out at  $T_0 = 181$  mK after the sample has been quenched from  $T_q = 796$  mK at  $H_q = 13.5$  T or from  $T_q = 761$  mK at  $H_q = 10$  T. To remove uninteresting contributions coming from the magnetocaloric effect and eddy-current heating, the measurements are repeated without temperature quenching, and the control data thus obtained are subtracted from the original data. The relaxation

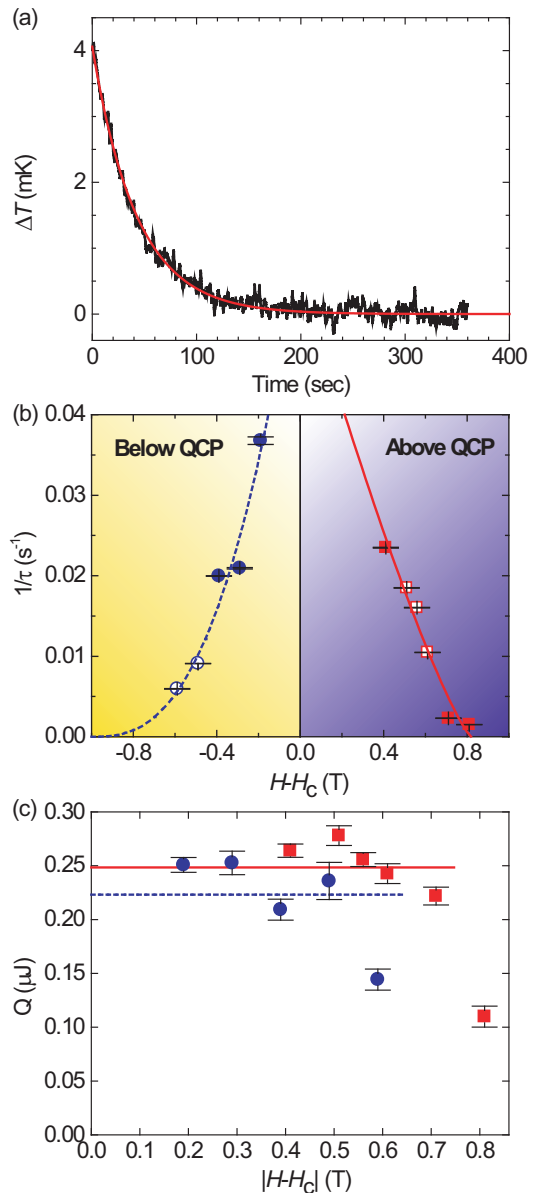


FIG. 4: (color online). Relaxation of the temperature difference between the sample and the thermal reservoir, as the magnetic field is brought close to  $H_c$  after temperature quenching to  $T_0 = 181$  mK. (a) Relaxation curve after a downward field sweep from  $H_q = 13.5$  T toward  $H_c$  at 0.1 T/min has been stopped at 12.7 T. The sample has been prepared by quenching it from  $T_q = 796$  mK at  $H_q$ . The line is a fit to an exponential relaxation with  $\tau = 42.6$  s. (b) Relaxation rate  $1/\tau$  vs. the field at which field sweep has been stopped. Solid symbols are data from curves showing exponential relaxation, and open symbols from curves showing stretched-exponential relaxation. Lines are guides to the eye. (c) Amount of heat released vs. the distance from  $H_c$ . Horizontal lines indicate the amounts of heat released during complete field sweeps through  $H_c$ . In (b) and (c), circles and broken lines are for  $T_q = 761$  mK at  $H_q = 10$  T, and squares and solid lines for  $T_q = 796$  mK at  $H_q = 13.5$  T.

is exponential at some  $H$  as shown in Fig. 4(a) but shows stretched-exponential behavior at other  $H$ , with the stretching exponent ranging from 0.61 to 0.78. The relaxation rate  $1/\tau$  diverges as the field approaches  $H_c$ , as shown in Fig. 4(b), indicating that diverging quantum fluctuations of the Cr(IV) spins near the QCP drive the relaxation of the nuclear spins. The divergence is asymmetric around  $H_c$ , faster for  $H > H_c$  than for  $H < H_c$ . This asymmetry is also seen in Fig. 3 as a wider quantum critical region for  $H > H_c$  than for  $H < H_c$ .

The amount of heat released during the relaxation-time measurements is shown as a function of  $|H - H_c|$  in Fig. 4(c). The result suggests that the ten hydrogen spins that release heat at this temperature contain two groups, each comprising four to six spins per formula unit. Above  $H_c$ , one group relaxes at  $|H - H_c|$  of about 0.8 T, whereas the other group relaxes at fields closer to  $H_c$ . Similarly, below  $H_c$ , the first group relaxes at  $|H - H_c|$  of about 0.6 T, whereas the second group relaxes at fields closer to  $H_c$ . The result is consistent with the molecular structure of Cr(diethylenetriamine)(O<sub>2</sub>)<sub>2</sub> shown in Fig. 1(a): the eight hydrogens bonded to the four carbons — with longer nuclear-spin  $\tau$  — fall into two groups, each consisting of four hydrogens, with distinct ranges of distances from the Cr(IV) [22].

In conclusion, our results provide unambiguous evidence that temperature quenching of Cr(dien) leaves the hydrogen nuclear spins frozen in a nonequilibrium high-energy state and, as the magnetic field is then brought close to the QCP, quantum fluctuations of the Cr(IV) ionic spins quickly anneal them to reach thermal equilibrium with the lattice. These results also imply that the quantum-fluctuation-driven heat release from nuclear spins is a generic phenomenon to be found near a variety of QCP. Because of the inextricable link between dynamic and static properties in quantum criticality, quantum-critical systems are predicted to exhibit interesting, non-trivial relaxation phenomena during and after a sweep of a control parameter such as magnetic field and pressure through the QCP [26] and also after temperature quenching near the QCP [27]. Our results warn, however, that the response of nuclear spins — which are nearly ubiquitous — to those changing parameters and to quantum fluctuations must be carefully taken into account in real solids. At the same time, heat release from nuclear spins promises to be a useful probe for the dynamics of quantum fluctuations that underlie quantum criticality in a variety of systems.

We thank S. Nellutla and A. Kumar for contributions to an early stage of this work and K. Ingersent, P. Kumar, Y. Lee, D. L. Maslov, and R. Saha for useful discussions. Thanks are also due to J.-H. Park, T. P. Murphy, and G. E. Jones for assistance and R. J. Clark for drawing a figure. This work was supported in part by NSF grant NIRT-DMR-0506946 and by the University of Florida Physics REU program under NSF grant DMR-

0552726. The experiment was performed at the National High Magnetic Field Laboratory, which is supported by NSF Cooperative Agreement DMR-0654118, by the State of Florida, and by the Department of Energy.

- 
- [1] J. A. Hertz, Phys. Rev. B **14**, 1165 (1976).
  - [2] S. Sachdev, *Quantum Phase Transitions* (Cambridge Univ. Press, Cambridge, 1999).
  - [3] H. v. Löhneysen, A. Rosch, M. Vojta, and P. Wölfle, Rev. Mod. Phys. **79**, 1015 (2007).
  - [4] P. Gegenwart, Q. Si, and F. Steglich, Nat. Phys. **4**, 186 (2008).
  - [5] N. D. Mathur *et al.*, Nature **394**, 39 (1998).
  - [6] H. Q. Yuan *et al.*, Science **302**, 2104 (2003).
  - [7] E. Fradkin and S. A. Kivelson, Phys. Rev. B **59**, 8065 (1999).
  - [8] M. P. Lilly *et al.*, Phys. Rev. Lett. **82**, 394 (1999).
  - [9] R. A. Borzi *et al.*, Science **315**, 214 (2007).
  - [10] Y. S. Oh *et al.*, Phys. Rev. Lett. **98**, 016401 (2007).
  - [11] C. Domb, *The Critical Point: a Historical Introduction to the Modern Theory of Critical Phenomena* (Taylor & Francis, London, 1996).
  - [12] S. L. Sondhi, S. M. Girvin, J. P. Carini, and D. Shahar, Rev. Mod. Phys. **69**, 315 (1997).
  - [13] Q. Si, Adv. Solid State Phys. **44**, 253 (2004).
  - [14] J. Brooke, D. Bitko, T. F. Rosenbaum, and G. Aeppli, Science **284**, 779 (1999).
  - [15] G. E. Santoro, R. Martonák, E. Tosatti, and R. Car, Science **295**, 2427 (2002).
  - [16] D. A. House and C. S. Garner, Nature **208**, 776 (1965).
  - [17] C. M. Ramsey *et al.*, Chem. Mater. **15**, 92 (2003).
  - [18] H. Tsujii *et al.*, Physica B **329–333**, 1638 (2003).
  - [19] The thermometers of the calorimeter have been self-calibrated in magnetic fields, by measuring the heat capacities of standard materials in situ. In the field range of the present experiment, calibration uncertainties are about 1.0% at 0.8 K and about 1.8% at 0.1 K.
  - [20]  $\Delta T$  during the subsequent sweeps, exhibiting only the magnetocaloric effect of at most 1 mK and eddy-current heating by 8 mK ( $T_0 = 181$  mK) and 3 mK ( $T_0 = 96$  mK), have been subtracted from the data shown in Figs. 1 and 2.
  - [21] For those points, 1.4 min of waiting is probably insufficient to thermalize the hydrogen nuclear spins.
  - [22] The five hydrogens bonded to the nitrogens are located at 2.40–2.52 Å from the Cr(IV), whereas the eight that are bonded to the carbons fall into two groups of four, each at 3.08–3.29 Å and 3.77–3.79 Å from the Cr(IV). The water hydrogens are at 3.29 and 3.48 Å from the closest Cr(IV) ions, which are in Cr(diethylenetriamine)(O<sub>2</sub>)<sub>2</sub> molecules not shown in Fig. 1(a). See supporting online information for Ref. [17].
  - [23] The peak position depends slightly on the quenching conditions  $T_q$  and  $H_q$ . For the data shown in Fig. 3, in the highly polarized paramagnetic phase,  $H_q = 13.5$  T and  $T_q = 0.80$  K except for the 227 mK point for which  $T_q = 1.04$  K. For those in the antiferromagnetically ordered phase,  $H_q = 9–10.5$  T and  $T_q = 0.76$  K except for the 226 mK point ( $T_q = 1.00$  K) and the 201 mK point taken at 0.2 T/min ( $T_q = 0.50$  K).

- [24]  $\tau$  measured in this manner is approximately  $T_1 + C_n/\kappa$  [25], where  $T_1$  is the nuclear spin-lattice relaxation time and  $C_n$  the nuclear heat capacity. At 181 mK,  $C_n/\kappa = 11.1$  s at 12.1 T.
- [25] B. Andraka and Y. Takano, *Rev. Sci. Instrum.* **67**, 4256 (1996).
- [26] D. Patanè *et al.*, *Phys. Rev. Lett.* **101**, 175701 (2008).
- [27] D. Patanè, A. Silva, F. Sols, and L. Amico, *Phys. Rev. Lett.* **102**, 245701 (2009).